13

Benchmarking of composite forming modelling techniques

J L GORCZYCA-COLE and J CHEN, University of Massachusetts Lowell, USA and J CAO, Northwestern University, USA

13.1 Introduction

Woven-fabric reinforced composites (hereafter referred to as woven composites) have attracted a significant amount of attention from both industry and academia, due to their high specific strength and stiffness as well as their supreme formability characteristics. However, applications of these materials have been hampered by a lack of low-cost fabrication methods, as well as robust simulation methods. Designing low-cost manufacturing processes requires accurate material modeling and process simulation tools. Recognizing these requirements, a group of international researchers gathered at the University of Massachusetts Lowell for the NSF Workshop on Composite Sheet Forming in September 2001. The main objectives of that workshop were to better understand the state-of-the-art and existing challenges in both materials characterization and numerical methods required for robust simulations of forming processes. One direct outcome of the workshop and the effort to move towards standardization of material characterization methods was a web-based forum exclusively for research on forming of woven composites, established in September 2003, at http://nwbenchmark.gtwebsolutions.com/. Other outcomes of the workshop are in the form of publications, such as this one, highlighting recommended practices for experimental techniques and modeling methods.

Material property characterization and material forming characterization were two main areas related to material testing identified at the 2001 NSF Composite Sheet Forming Workshop. Standard material testing methods are necessary for researchers to understand the formability of the material, the effect of process variables on formability, and to provide input data and validation data for numerical simulations. Thus, the researchers embarked on a benchmarking project to study, understand and report the results of material testing efforts currently in use around the world for woven composites to make recommendations for best practices.

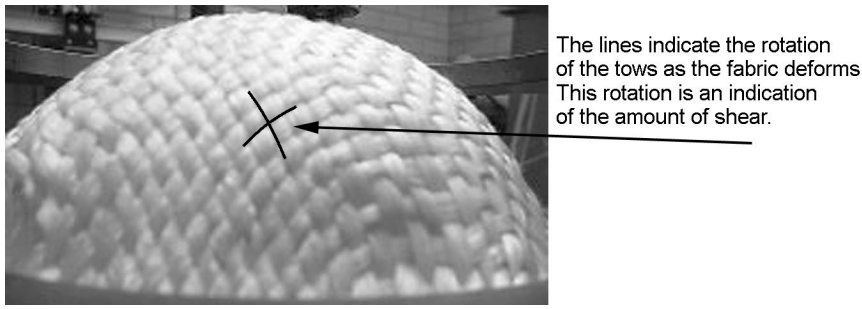

13.1 Fabric shearing.

Three different commingled fiberglass-polypropylene woven-composite materials were used for this research. The materials were donated by Vetrotex Saint-Gobain in May 2003 and were distributed in July 2003 to the following research groups: Hong Kong University of Science and Technology (HKUST) in Hong Kong, Katholieke Universiteit Leuven (KUL) in Belgium, Laboratoire de Mécanique des Systèmes et des Procédés (LMSP) in France, Northwestern University (NU) in the USA, University of Massachusetts Lowell (UML) in the USA and University of Twente (UT) in the Netherlands.

As intra-ply shear is the most dominant deformation mode in woven composite forming (Fig. 13.1), the trellis-frame (picture-frame) test (Fig. 13.2) and the bias-extension test (Fig. 13.3) were identified for further study related to material shear-property characterization. This paper focuses on the shear property determined from the results of the trellis-frame-test. Five of the six research groups listed submitted data for the experimental trellising-shear part of the benchmark project. A summary and comparison of the trellis-frame test methods and the findings from all participating research groups is presented. Future publications will focus on the bias-extension results.

A summary of the properties of the materials used in this study is presented in Section 13.2. More detailed information about the fabric is also listed on the forum website. Trellis-frame-test results along with the experimental techniques

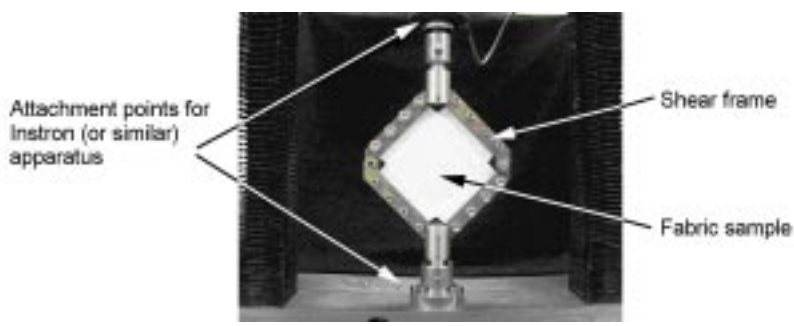

13.2 Trellising-shear test apparatus.

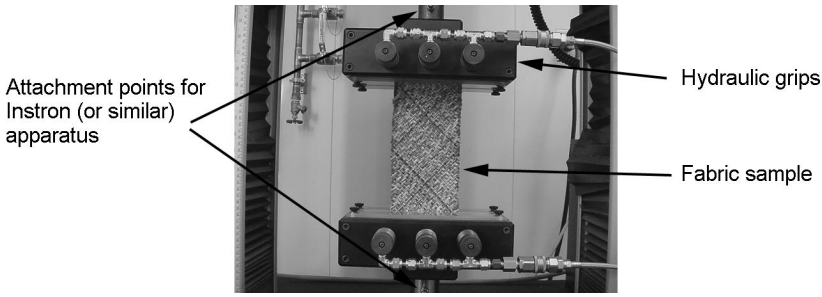

13.3 Bias-extension test apparatus.

are the focus of Section 13.3. Also, all the data reported are available for download at the forum website. Section 13.4 discusses how the data from these tests can be used to advance the benchmarking effort related to the numerical modeling of the benchmark fabrics in thermostamping simulations. Conclusions and future work are presented in Section 13.5.

13.2 Forming process and fabric properties

As stated in the introduction, the three types of woven fabrics used in this study were donated by Vetrotex Saint-Gobain (Fig. 13.4). The fabric properties, as reported by the material supplier and benchmark participants, are listed in Table 13.1. Each fabric is comprised of yarns with continuous commingled glass and polypropylene (PP) fibers. These fabrics were chosen due to their ability to be formed using the thermostamping method.

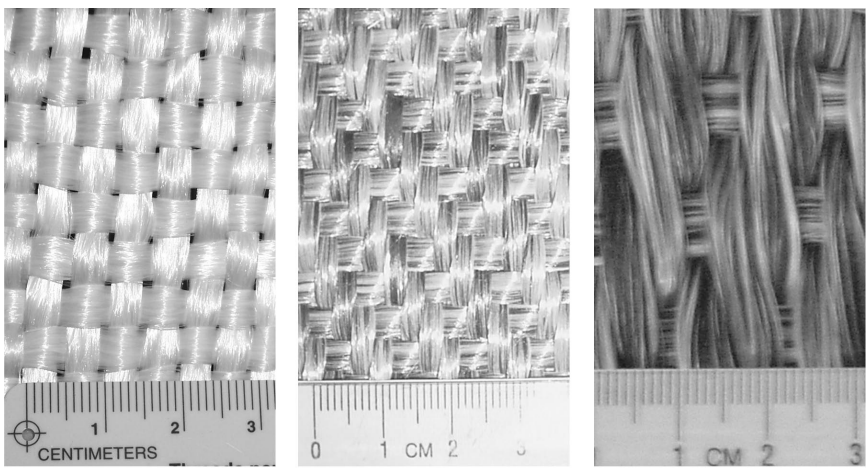

(a) Plain weave (b) Balanced twill weave (c) Unbalanced twill weave

13.4 Woven fabrics tested.

Table 13.1 Fabric parameters (as reported by the material supplier unless specified otherwise)

	TPEET22XXX	TPEET44XXX	TPECU53XXX
Manufacturer's style			
Weave type	Plain	Balanced twill	Unbalanced twill
Yarns	Glass/PP	Glass/PP	Glass/PP
Weave	Plain	Twill 2/2	Twill 2/2
Areal density, g/m^2	743	1485	1816
Yarn linear density, tex	1870	1870	2400
Thickness*, mm	1.2 (NU)	2.0 (NU)	3.3 (NU)
Yarn count, picks/cm or ends/cm			
Warp	1.91 (KUL) 1.93 (HKUST) 1.95 (NU)	5.56 (KUL)	3.39 (KUL)
Weft	1.90 (KUL) 1.93 (HKUST) 1.95 (NU)	3.75 (KUL)	1.52 (KUL)
Yarn width in the fabric, mm (standard deviation)**			
Warp	4.18 ± 0.140** (KUL) 4.20 (HKUST) 4.27 (NU)	1.62 ± 0.107** (KUL)	2.72 ± 0.38** (KUL)
Weft	4.22 ± 0.150** (KUL) 4.20 (HKUST) 4.27 (NU)	2.32 ± 0.401** (KUL)	3.58 ± 0.21** (KUL)

* ASTM Standard D1777 (Applied pressure = 4.14 kPa)

For commingled woven fabrics, the thermostamping process is a rapid manufacturing method similar to the stamping method used to form metal parts. The main difference between the thermostamping process and stamping process is the addition of heat. An oven is present at the start of the forming process to heat the fabric blank. The tools are also heated in the thermostamping process so that the fabric blank does not cool before it is fully formed. Recall from the introduction that the objective of the thermostamping process is the reorientation of the yarns through rotation or shearing to produce the desired shape from a fabric blank (Fig. 13.1). Any wrinkling present in the final part would indicate a defect. In the oven, the fabric is heated above 165°C to melt the PP fibers. When the fabric blank leaves the oven it is placed beneath a punch. A binder is rapidly placed over the fabric blank to apply in-plane tension to the yarns. This tension aids in the prevention of wrinkling during the stamping process by causing the yarns in the fabric to rotate and take on the shape of the die. The punch then presses the fabric into a die. The metal tools are heated to slow the rate at which

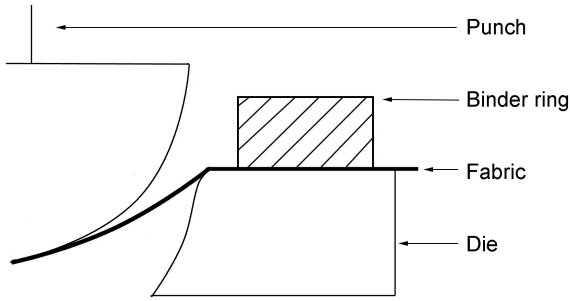

13.5 Schematic of thermostamping components.

the PP cools and solidifies (Fig. 13.5). In the final formed part, the glass fibers act as the reinforcement to the PP matrix. A schematic of the process is shown in Fig. 13.5.

13.3 Experimental

A trellis frame or picture frame is a fixture used to perform a shear test for woven fabrics. As stated in the introduction, the test procedures used by the participating researchers were not identical. However, the tests were equivalent in principle. As recommendations for best practices and standardized test procedures were one of the desired outcomes of this research, researchers did not limit all groups to perform the test using the exact same procedure. By using varying procedures researchers could study and recommend methods for data comparison.

Before discussing the test procedure in detail, it should be noted that some groups chose not to submit results for all of the fabrics included in this study. Table 13.2 shows the fabrics tested by each participant.

All researchers reported load histories and global-shear-angle data for picture-frame tests conducted at room temperature. The researchers decided that even though temperature effects were an important part of the process, initial

Table 13.2 Tested fabrics by participating researchers

Group	Plain weave	Balanced twill weave	Unbalanced twill weave
HKUST	Y	N	N
KUL	Y	Y	Y
LMSP	Y	Y	Y
UML	Y	Y	Y
UT	Y	Y	N

Note: (Y = data reported; N = data not reported)

comparisons among results obtained using non-standard test procedures should be conducted without varying the temperature. Once the differences were understood at room temperature, the additional complexity of comparing results at elevated temperatures would be incorporated into the study.

One main difference in the procedure used by the five groups who submitted results can be observed in the type of frame used. Although the frames used in this study are not identical (Fig. 13.6, Table 13.2), all of them have common features. For example, the corners of each frame are pinned. When the fabric is loaded into the frame, it is clamped on all edges to prevent slippage. The corners are cut out of the sample to allow the tows to rotate without wrinkling the fabric. Thus, it appears that each sample has four flanges (Fig. 13.6). The

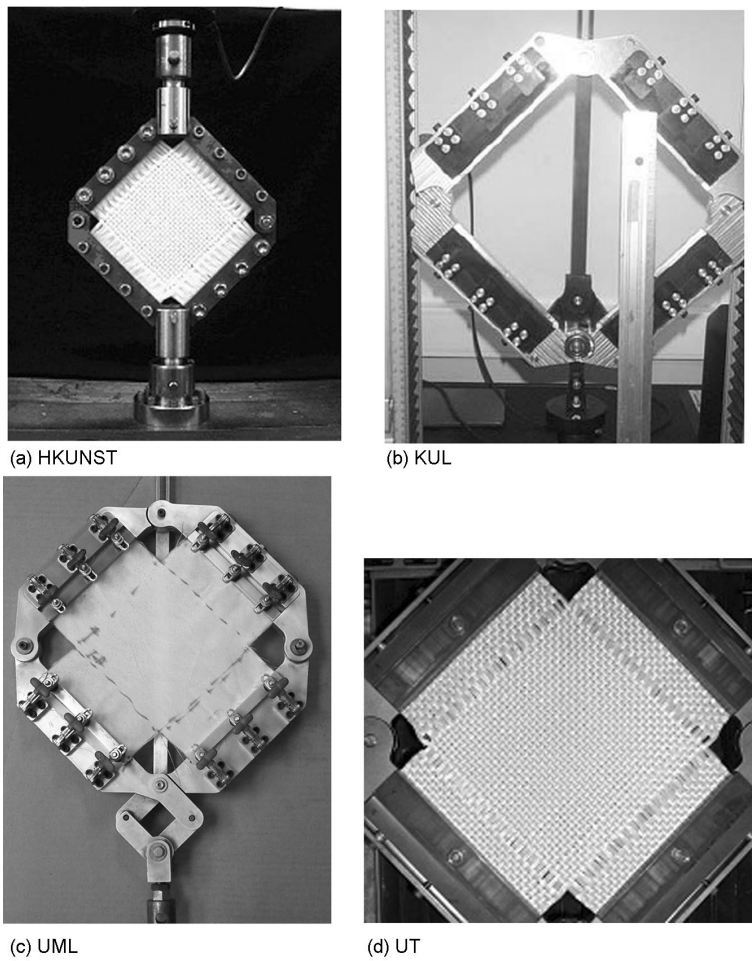

13.6 Picture frames designed, fabricated and used by the research groups.

sample size is considered to be the area of the fabric without the flanges as that area represents the amount of fabric that is deformed during the test. It is the area that encompasses the tows which must rotate at the crossover points during the test.

One may also note different clamping mechanisms in Fig. 13.6. It was assumed that all clamping mechanisms held the fabric rigidly in the frame and there was no slippage. Thus, differences in clamping mechanisms are not taken into account in the analysis of the results. With the fabric properly aligned and tightly clamped in the frame, the distance between two opposing corners is increased with the aid of an Instron testing machine (or similar tensile test apparatus). Figure 13.7 shows a fabric sample loaded in a picture frame in the starting position and in the deformed position. Using this test method uniform shearing of the majority of the fabric specimen is obtained. Displacement and load data are recorded to aid in the characterization of pure shear behavior. The operating principles of each frame are the same in that the fabric sample is initially square (Table 13.3) and the tows are oriented in the 0/90 position to start the test (Figs 13.6 and 13.7). Also, after the test begins and the crosshead displacement increases, pulling on the frame, the tows begin to reorient themselves as they shear (Fig. 13.7). However, the mechanism by which the fabric deforms is aided by linkages in the frames used by KUL and UML (Fig.

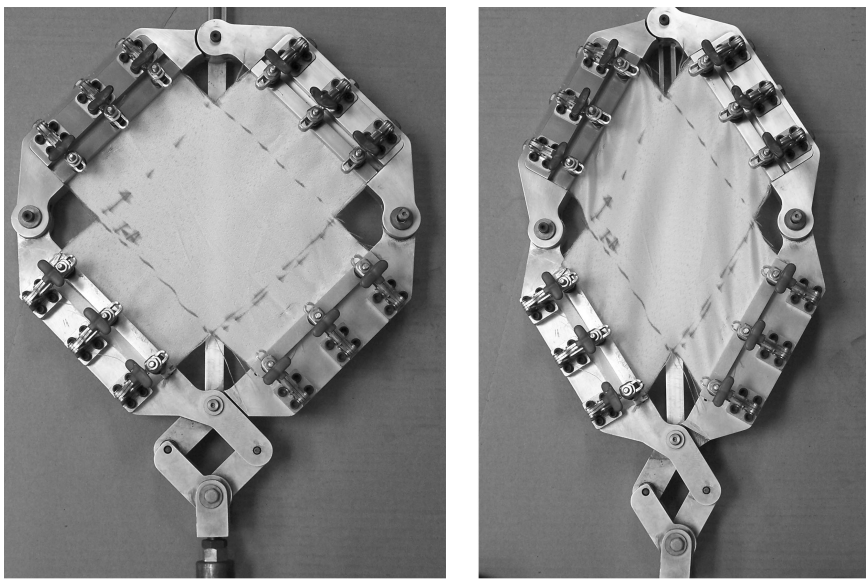

13.7 UML shear frame (a) starting position (b) deformed position. (Note that the top hinge has traveled from the bottom of the slot in the undeformed position (a) to the top of the slot in the deformed position (b).)

Table 13.3 Frame size and test parameters

Group	Frame (mm)	Fabric (mm)	Speed (mm/min)	Specimen temperature
HKUST	180	140	10	Room temperature
KUL	250	180	20	
LMSP	245	240	75 to 450	
UML	216	140	120	
UT	250	180	1000	

13.6). UML's linkage was added to allow the frame to displace a greater speed than could be achieved by the Instron or tensile test machine alone. Note the inclusion of the slot in the KUL and UML frames (Figs 13.6–13.8). In addition to amplifying the distance traveled, these linkages amplify the measured force, and this amplification factor must be accounted for when the results from all the groups are analyzed and compared. When this amplification factor was removed, it was expected that the results from different groups would be comparable if a proper normalization technique was used to account for differences in sample and frame size. A detailed discussion of the amplification factor associated with the inclusion of the linkages and the various normalization techniques is included in the discussion of results. This section focuses on the similarities and differences of the test methods used by each group.

Additional differences in the test procedure among the groups were related to sample preparation. For example, to eliminate the potential force contribution from shearing of the yarns in the edge (arm) parts of the sample, HKUST removed all of the unclamped fringe yarns (Fig. 13.9). UT reported that they removed some of the yarns adjacent to the center area of the sample to prevent the material from wrinkling during testing (Fig. 13.9). In previous research by

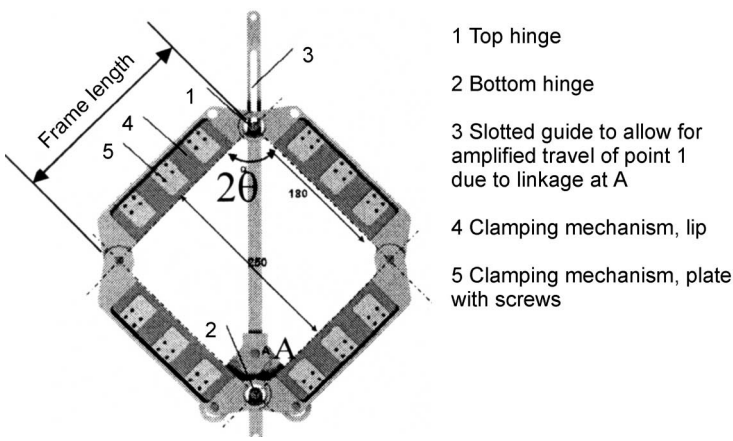

13.8 Schematic of picture frame (KUL).

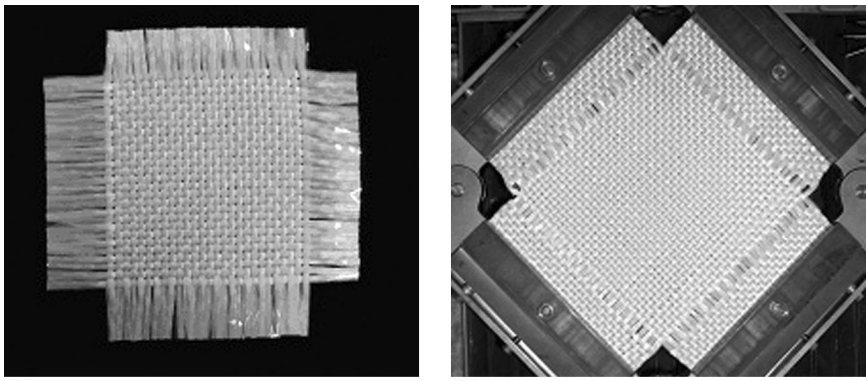

13.9 Specimens with yarns removed from arm regions (a) HKUST (b) UT.

Lussier (2000), it was reported that care must be taken not to alter the tightness of the weave or local orientation of the remaining yarns when removing some of the yarns prior to testing the fabric. This statement was further supported by HKUST who noted that theoretically in an obliquely oriented or misaligned specimen in the frame, one group of yarns would be under tension while the other would be under compression. Because a yarn cannot be compressed in the longitudinal direction, a misalignment would indicate that the yarn buckles out of the original plane and the onset of wrinkling in the fabric occurs at lower shear angles than when the specimen is properly aligned in the frame.

UT terminated their tests at the onset of wrinkling, as the shear deformation is no longer uniform once wrinkling occurs. UML noted that by 'mechanically conditioning' the specimen, i.e., by shearing the fabric in the frame several times before starting the test the variability in tension due to local deviations in orientation could be eliminated. This occurrence indicates the importance of the precise handling of both the sample and test fixture.

Figure 13.8 shows a schematic drawing of a picture frame. In this case, a displacement transducer in the tensile machine measures the vertical displacement, d, of point A (KUL, UT). Through trigonometric relations, the angle of the frame, θ, is calculated.

$$\cos\theta = \frac{\sqrt{2}L_{frame} + d}{2 \times L_{frame}} \qquad 13.1$$

where L_{frame} is the frame length indicated in Fig. 13.8. The shear angle, γ, is calculated from the geometry of the picture frame.

$$\gamma = 90^\circ - 2\theta \qquad 13.2$$

This value, γ, is also called the global shear angle. Note that this value is taken to be an average shear value over the entire specimen. The actual shear angle at

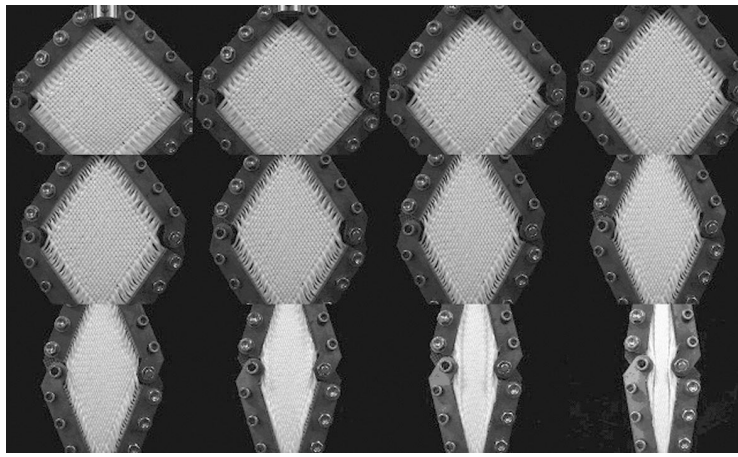

13.10 Array of images captured during the loading process (HKUST).

any point on the fabric may vary. (HKUST and UML used a similar approach to determine γ based on their displacement measurements.)

Optical methods which can aid in the determination of the shear angle at any particular point on the fabric specimen also exist. HKUST used a camera to capture arrays of images during the loading process. They then processed these images with AutoCAD, as shown in Figs 13.10 and 13.11. They found that the maximum deviation between the measured shear angle and the calculated shear angle (Eq. 13.2) is about 9.3% and that the maximum deviation typically occurs at larger shear angles. Based upon the small percent difference, the shear angle reported in this paper is the calculated shear angle. Thus, the shear angle is consistent with the method used by the other research groups.

KUL incorporated an image mapping system (Aramis) into their experiment. After photos were taken by a CCD camera, displacement and strain fields are identified by the Aramis software by analyzing the difference between two subsequent photos. Figure 13.12 shows a von Mises strain distribution over an image of a fabric sample during testing. By averaging the local shear angles

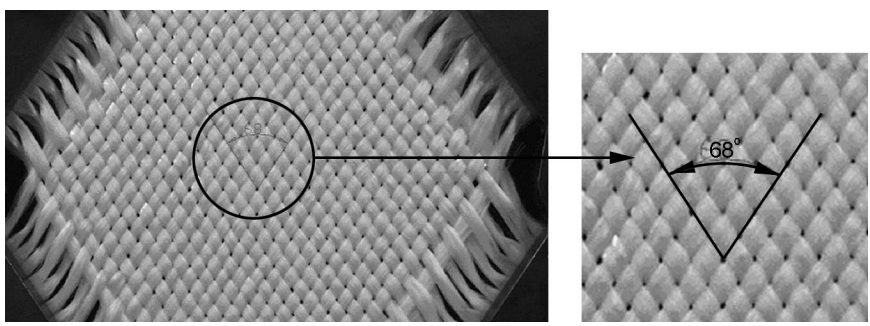

13.11 Shear angle measurement on a photo (HKUST).

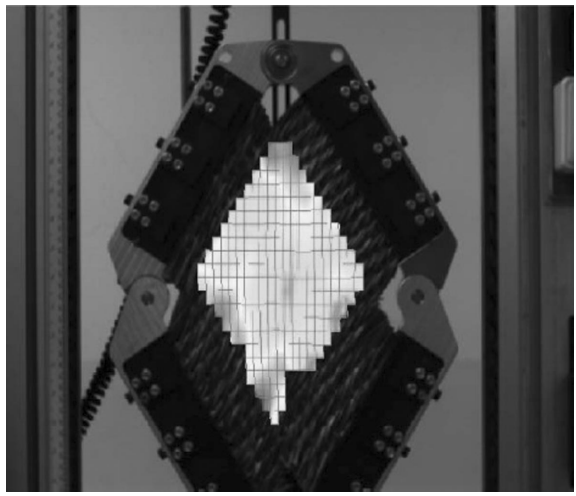

13.12 Image of the fabric and the central region with the von Mises strain field (KUL).

produced by Aramis and comparing them with the global shear angles calculated from the crosshead displacement using Eqs. 13.1 and 13.2, KUL generated the graph in Fig. 13.13, which shows that the shear angle values obtained using the two methods are comparable. Again, as the difference was small between the calculated shear angle and the shear angle measured with the mapping system as well as to be consistent with the groups participating in this study, the shear angle used in this paper is the shear angle calculated from the crosshead displacement.

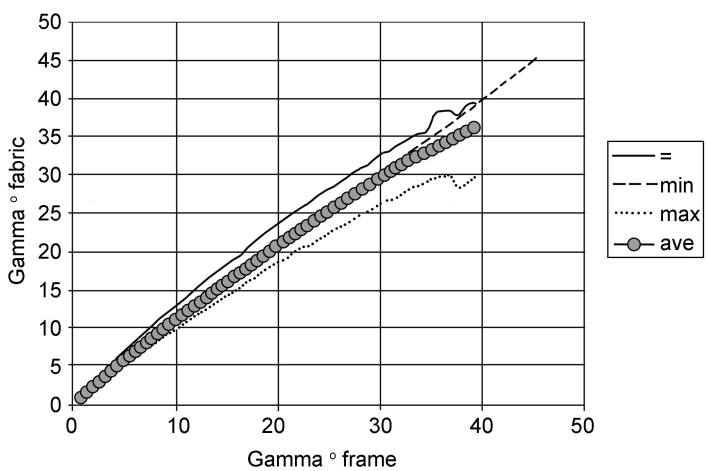

13.13 Typical relationship between the optically measured shear angle and shear angle of the frame, unbalanced twill weave (KUL).

The force needed to deform the fixture must be measured to accurately determine the actual force required to shear the fabric. HKUST and UML conducted several tests on their frames without including a fabric blank to record the force required to deform the frame, F'. This value was subtracted from the results obtained from fabric shear tests F''. The difference in these values is the force required to shear the fabric sample. Shear force, F_s, is calculated,

$$F_s = \frac{F}{2\cos\theta} = \frac{F'' - F'}{2\cos\theta} \qquad 13.3$$

where F is the load after subtracting a constant offset value from each data point to eliminate the error caused by the weight and inertia of the fixture, and θ is the angle shown in Fig. 13.8 calculated using Eq. 13.1.

KUL used a different method to measure the force required to deform the fixture, F'. Their method required a hinge (Fig. 13.14) to balance the initial weight and calibrate the results under various loading speeds.

After subtracting the offset force, F', from the measured force value, F'', the shear force, F_s, may be calculated with the aid of the frame geometry and a free-body diagram.

$$F_s = \frac{F}{2\cos\theta} = \frac{F'' - F'}{2\cos\theta} \qquad 13.4$$

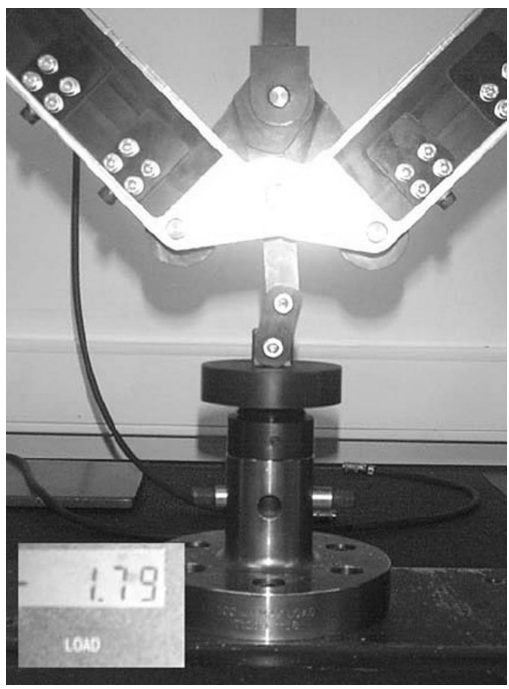

13.14 Hinge for calibrating the force required to deform the frame.

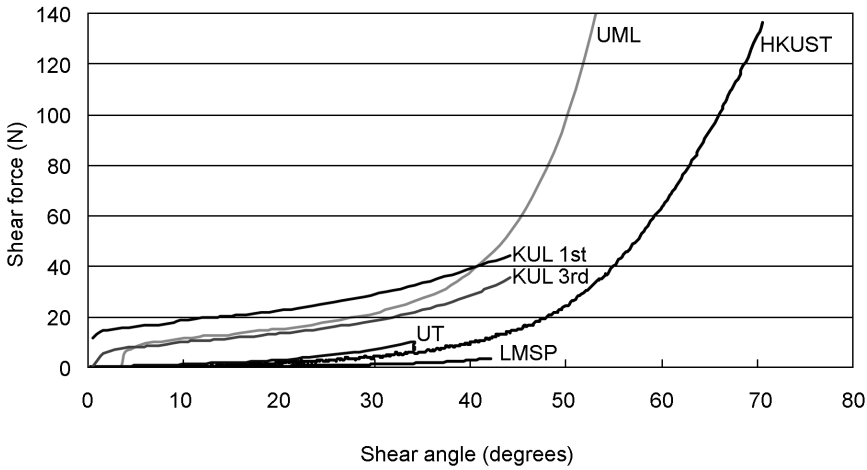

13.15 Shear force versus shear angle.

Figure 13.15 shows shear-force data as a function of the calculated shear angle (Eq. 13.2) for plain-weave fabric at room temperature. Shear forces are calculated based on the tensile machine loads according to Eqs. 13.3 and 13.4.

Based solely on Fig. 13.15, the data obtained for the shear force does not seem to be comparable. However, the differences among the frames and the sample sizes have not yet been taken into account. The following paragraphs will explain methods for comparing shear frame data obtained by different groups using different shear frames and different samples sizes. The first difference which should be accounted for is the inclusion of a linkage on the test frame. Note that KUL and UML both use shear frames with a linkage, while the other groups do not have a linkage on their shear frames. This linkage was included by UML because they needed to run the tests at a speed higher than their Instron machine could accommodate. By including the linkage and the slot, the frame could travel at a rate 4.25 times faster than was possible through the specified crosshead displacement rate. From these experiments, it has been found that the linkage introduces an amplification factor in the force calculation. Thus, to compare data when some groups have a shear frame with a linkage to the data from other groups whose shear frame does not have a linkage, the amplification factor must be removed.

Using UML's frame for the picture frame tests, the displacement and load are applied on the corner of the small amplifier frame marked 'A' instead of on the top corner of frame that clamps the fabric (Fig. 13.16). Note that point 'A' is the point at which the sliding link attaches the crosshead mount to the amplifier linkage. Therefore, a kinematic analysis of the picture frame with the amplifier is necessary for the calculation of the shear angle and shear load in the test. When performing this analysis, it should be noted that the amplifier shares two

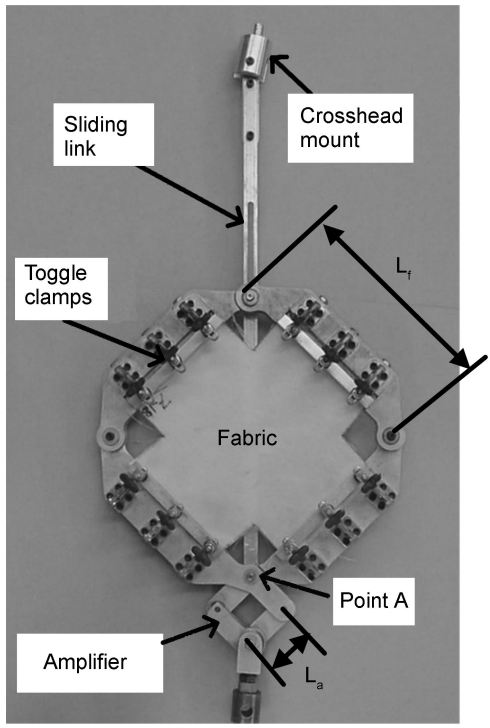

13.16 Trellis-frame test fixture (UML).

pieces of the frame with the picture frame, arms B and C. Thus, the shear angle of the amplifier equals the shear angle of the picture frame.

Beginning with the geometry of the amplifier frame, as shown in Fig. 13.17, the displacement of point 'A', δ_a, can be calculated.

$$\delta_a = 2L_a\left(\cos\left(\frac{\pi}{4} - \frac{\gamma}{2}\right) - \frac{\sqrt{2}}{2}\right) \qquad 13.5$$

where L_a is the length of one side of the amplifier frame and γ is the shear angle.

Solving Eq. 13.5 for the shear angle, γ,

$$\gamma = \frac{\pi}{2} - 2\cos^{-1}\left(\frac{\delta_a}{2L_a} + \frac{\sqrt{2}}{2}\right) \qquad 13.6$$

To calculate the shear load, the kinematics of the picture frame is studied. Figure 13.17 shows the schematic diagram of the picture frame. The free body diagrams of the side frame BC and BAF are shown in Fig. 13.18.

From Fig. 13.18, note that joint *C* is free for motion. Using symmetry, it can be determined that the force applied on joint *C* from link *CD* and *BC* is zero. Thus, performing a static analysis using the free body diagram of link *BC* (Fig. 13.19a),

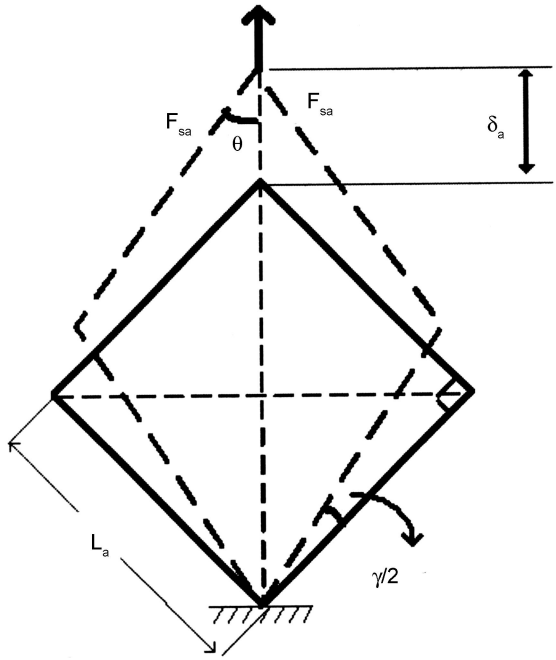

13.17 Geometry of the amplifier.

$$F_B - F_s = 0 \quad \text{or} \quad F_B = F_s \tag{13.7}$$

where F_B is the force on joint B between link BC and link BAF and F_s is the shear force the fabric sample applied to link BC.

Then, from the free body diagram of link BAF in Fig. 13.19b,

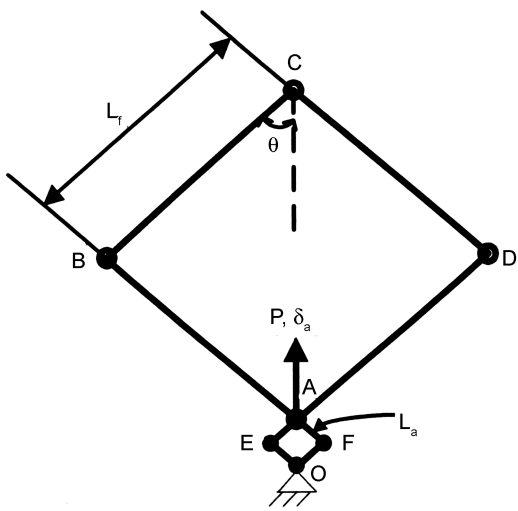

13.18 Schematic diagram of the picture frame at UML.

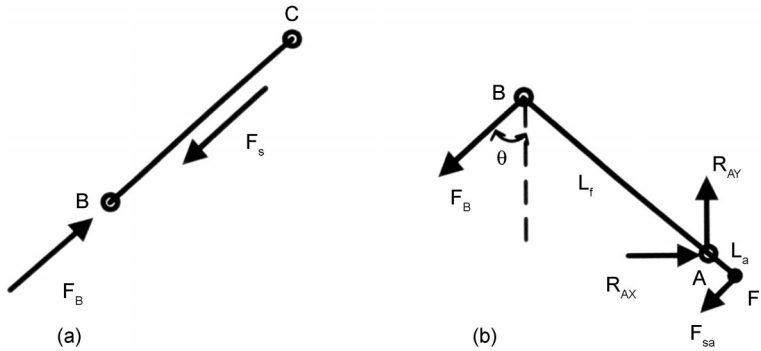

13.19 Free body diagrams of (a) link BC, and (b) link BAF.

$$M_A = 0 \quad \text{or} \quad F_B L_f \sin(2\theta) - F_{sa} L_a \sin(2\theta) = 0 \tag{13.8}$$

where M_A is the moment at point A, L_f is the length of link BC, F_{sa} is the shear force applied on the amplifier frame from the Instron machine and θ is the angle between link BC to the vertical direction as seen in Fig. 13.4. Solving Eq. 13.8 for F_B,

$$F_B = \frac{F_{sa} L_a}{L_f} \tag{13.9}$$

Defining an amplification factor as, α,

$$\alpha = \frac{L_f}{L_a} \tag{13.10}$$

From the geometry of the amplifier frame, the shear force of the amplifier, F_{sa}, can be calculated.

$$F_{sa} = \frac{P}{2\cos\theta} \tag{13.11}$$

where P is the force measured on the load cell in the crosshead.

Substituting Eqs. 13.7, 13.10 and 13.11 into Eq. 13.9,

$$F_s = \frac{P}{2\alpha\cos\theta} \tag{13.12}$$

Thus, in processing the picture frame test data at UML, Eqs. 13.6 and 13.11 are used to calculate the shear angle and the shear load, respectively. After comparing Eq. 13.12 with Eq. 13.3, it should be noted that the shear force equation is only altered through the inclusion of the amplification factor in the denominator in the left-hand side of the equation. Intuitively, this is reasonable because the amplification factor, α, for a frame with no amplification linkage would be 1 and Eq. 13.12 would then be equivalent to Eq. 13.3.

A similar analysis can be performed on the frame used by KUL. However, some differences exist because the amplification linkage in the KUL frame is

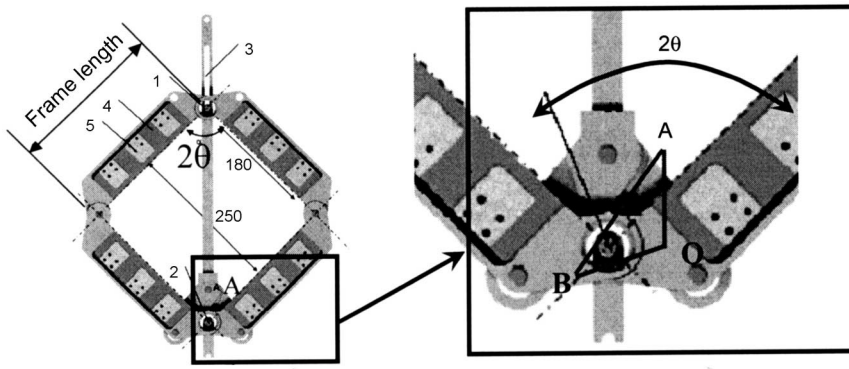

13.20 Geometry of picture frame (KUL).

inverted when compared to the amplification linkage in the UML frame (Figs 13.7 and 13.8). The geometry of the linkage in KUL's frame is shown in detail in Fig. 13.20. Note that none of the angles of the KUL amplification linkage are equal to the shear angle for the fabric as the crosshead moves in the vertical direction. Thus, the amplification factor for the KUL frame is not a constant value like it was for the UML frame. However, upon performing a kinematic analysis, an equation (as opposed to a constant value) can be determined for the amplification factor, α, and substituted into Eq. 13.12.

Figure 13.21 shows the data comparison with the amplification factor introduced by the linkages in the frames used by UML and KUL removed.

HKUST and UML mechanically conditioned the samples prior to testing, LMSP reported the results from the third repetition of the test on a single sample

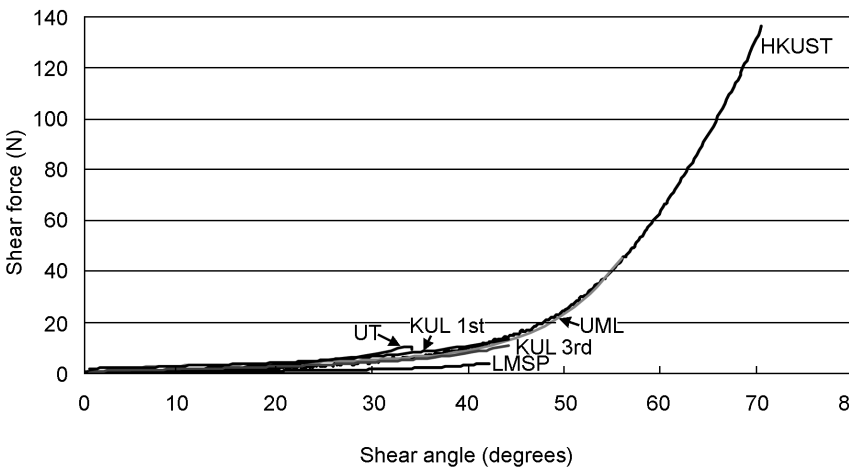

13.21 Shear force versus shear angle with linkage amplification removed from UML and KUL results.

and KUL reported data for each of three repetitions of the test on a single sample. Examining the data from the third repetition of the test on a single sample can be equated to mechanical conditioning, as the sample has deformed two times. KUL noted that the data from the second and third repetitions on a single sample were comparable with each other, but both were well below the data from the first time the sample was deformed in the shear frame. UT did not report whether their samples were mechanically conditioned prior to testing or that repeated tests were performed on the same samples at any time.

The calculations in the remainder of this report will focus on the region of the plot before 60º. It was at approximately 45º where locking began to occur for this fabric. Locking refers to the point at which the tows are no longer able to rotate and they begin to exert a compressive force on each other as the fabric is further deformed. The force required to deform the fabric begins to increase significantly as the locking angle is reached and surpassed. When the compression of the tows reaches a maximum, wrinkling begins to occur and the fabric begins to buckle out of plane. Wrinkling in a formed part is considered a defect. Thus, it is undesirable. Figure 13.22 shows the shear force vs. shear angle obtained from different groups up to 60º of shearing angle.

One proposed method for normalization was to use the frame length. Figure 13.23 presents the force results normalized by the length of the frame used by each group. As seen, the normalization brought curves closer, but noticeable deviations are still seen. Frame length could be indicative of sample size, i.e. a larger frame may indicate a larger sample size which in turn would indicate the deformation of a greater number of crossovers. However, as there is no standard ratio for the length of a test sample to the length of the frame, this method is not the best method for normalization.

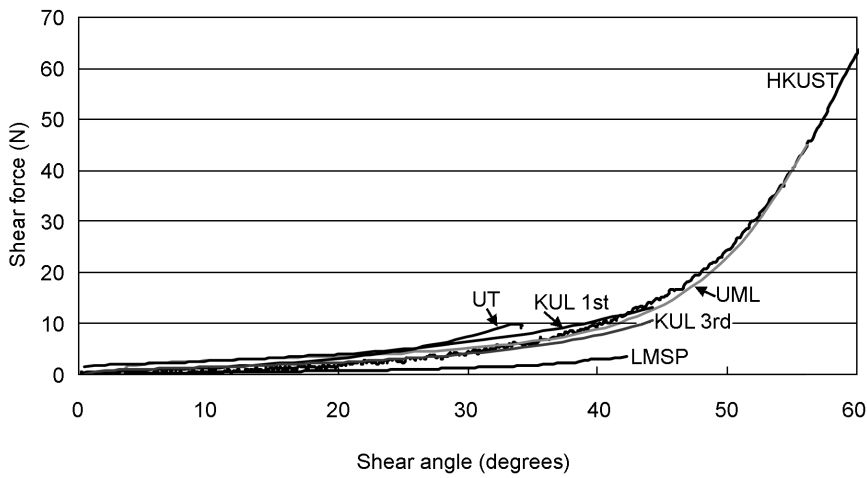

13.22 Shear force versus shear angle comparison prior to locking.

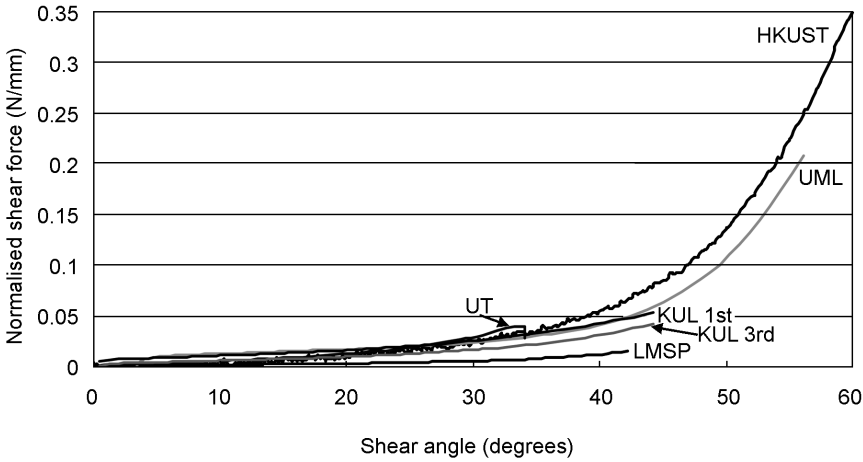

13.23 Shear force normalized by frame length versus shear angle.

The investigation continued by comparing the data when normalized by fabric area. For this research the fabric area was defined as the inner square area of the sample, i.e. the arms were neglected (Fig. 13.24). The fabric area would be related to the number of crossovers in the material. A larger sample would have more yarns resulting in more crossovers between the yarns. Figure 13.25 shows the results when the data was normalized by the fabric area. Again, this normalization technique brought the curves closer together, but researchers were interested in a more comprehensive normalization technique. A technique which took into account both the size of the sample and the size of the frame was then investigated.

Both Peng *et al.* (2004) and Harrison *et al.* (2004) have developed normalization methods using an energy method. Harrison *et al.* (2004) studied the case where the frame length is equal to the fabric length. They researched

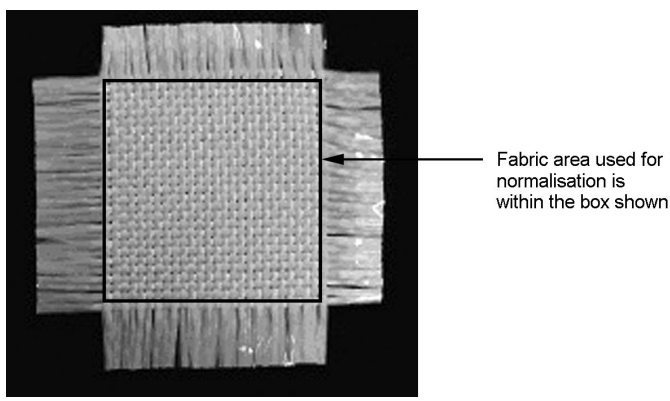

13.24 Sample area used for normalization.

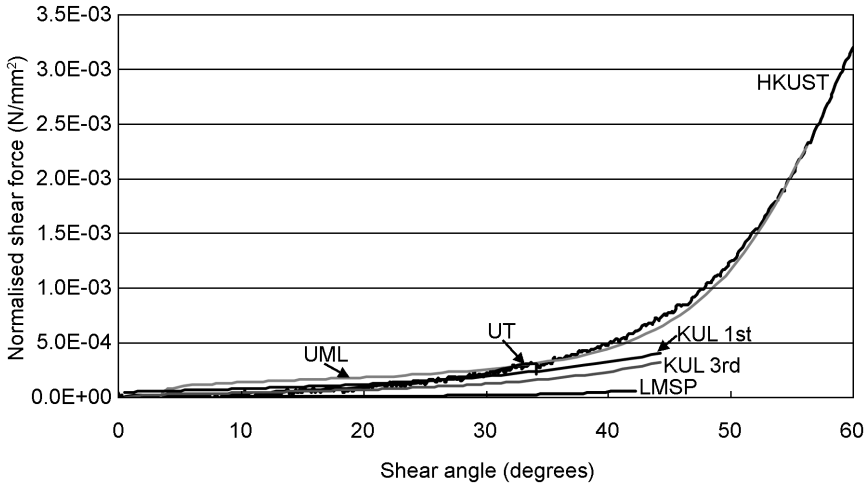

13.25 Shear force normalized by fabric area versus shear angle.

and proposed a method for comparing the force results obtained using shear frames (and as a result fabric samples) of different sizes. Peng *et al.* (2004) studied that case and the case where the length of the fabric sample is not equal to the length of the frame. Their equation reduces to the method proposed by Harrison *et al.* (2004) for the case when the fabric length is equal to the frame length. Thus, as proposed by Peng *et al.* (2004), to normalize the force data,

$$P_{normalized} = P_{original} \cdot \frac{L_{frame}}{L_{fabric}^2} \qquad 13.13$$

where $P_{normalized}$ is the shear force normalized according to the energy method, $P_{original}$ is the force required to shear the fabric, L_{frame} is the length of the frame and L_{fabric} is the length of the fabric.

When the length of the fabric is equal to the length of the frame, this equation becomes,

$$P_{normalized} = P_{original} \cdot \frac{1}{L_{frame}} = P_{original} \cdot \frac{1}{L_{fabric}} \qquad 13.14$$

as proposed by Harrison *et al.* (2004).

Figure 13.26 presents the normalized data using Eq. 13.13. Notice that the best agreement in the low shear angle region is obtained using this method when compared to normalizing the data by the frame size and the sample size independently.

In this section of the chapter, important features of the picture-frame test were presented, including: preparation of the samples, length definitions, force and shear angle measurements and calculations, repeatability, and comparison of

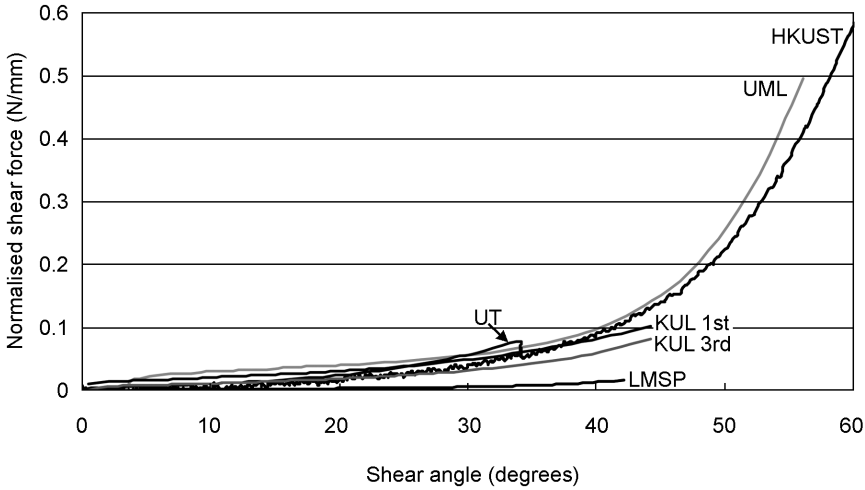

13.26 Shear force normalized using the energy method versus shear angle.

results force data with and without normalization methods. These normalization methods show that the results from different groups using different shear frames can be compared.

13.4 Numerical analyses

Researchers noted that repeatability of the experimental results was improved with tests performed on the same sample and with preconditioning. Researchers realize that fabric handling may decrease repeatability as well if the handling affects the alignment of the tows in the fabric. Thus, it may be feasible to incorporate a step into the manufacturing process that will precondition the sample or aid in the proper alignment of tows prior to the forming process. However, research has not been conducted to assess the actual impact of conditioning on the forming of a part. HKUST reported on the impact of misalignment of the fabric in the frame causing early onset of wrinkling. Again, misalignment of the fabric has not been investigated in relation to the forming of a part. One way to investigate these effects would be to stamp the actual parts and compare the results through visual inspections and experimental tests. However, realizing that this could be a costly and time-consuming process, the researchers involved with this project are continuing the benchmarking effort with a numerical forming investigation. The results from the shear tests will be used in that investigation as part of the constitutive material relations. The data from the benchmarking study of the shear behavior of the fabric can be incorporated into the numerical investigations currently underway in the benchmarking effort. The following paragraphs outline the proposed method for

determining the shear modulus of the fabric from the shear force normalized using the energy method (Eqs. 13.13 and 13.14). This shear modulus can be incorporated into finite element models of the thermostamping process through the use of a user-supplied material model. As more tests are performed on the fabric, the user-supplied material models can be updated to provide a more robust analysis of the forming behavior of the materials under investigation.

By definition, the shear stress, τ, is obtained by dividing force by cross-sectional area.

$$\tau = \frac{P_{original}}{Area} = \frac{P_{original}}{L_{fabric} \cdot t_{fabric}} \qquad 13.15$$

In Eq. 13.15, by definition, the cross-sectional area, denoted by the variable *Area*, is equal to the length of the fabric, L_{fabric}, multiplied by the thickness of the fabric, t_{fabric}. Note that the denominator in Eq. 13.15 contains L_{fabric}, as does the denominator of the normalized force in Eqs. 13.13 and 13.14. Thus, to calculate the shear stress using the force normalized by fabric length, it is only necessary to divide the normalized force by the thickness of the fabric, t_{fabric}, not the area not the cross-sectional area, *Area*. Hence, the shear stress is,

$$\tau = \frac{P_{normalised}}{t_{fabric}} \qquad 13.16$$

It is then proposed that the shear modulus can be calculated from the derivative of the regression equation determined from the data points on the shear stress versus shear strain plot, if the units of shear strain are in radians. These results are shown in Fig. 13.27. Note that there is little difference in the

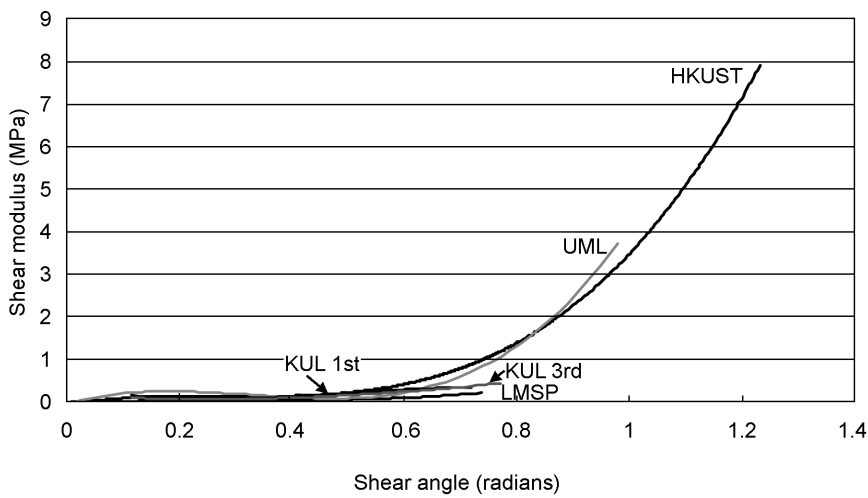

13.27 Shear modulus (MPa) versus shear angle (radians).

shear modulus among the groups until the locking angle is approached (i.e. where the shear modulus begins to rapidly increase). Thus, there should not be any significant differences in the modeling results for deformation in the region below the locking angle. However, only two groups collected data in the region where the shear modulus begins to rapidly increase as the locking angle is approached and exceeded. Thus, it is difficult to draw conclusions for this region. In future studies, such as those where the temperature effects will be considered, participating research groups should be asked to collect data over a wider range of angles so that more definite conclusions can be drawn.

13.5 Conclusions and future trends

The properties of woven fabrics are very different from conventional materials, such as bulk metals and polymers. This phenomenon lead to the interest in the woven-fabric composite material community to conduct benchmark tests. It has been shown that picture-frame tests are able to produce valuable experimental data for analytical and numerical research on woven composites. Mechanically conditioning the sample can also improve repeatability. This was shown through results from UML and KUL. UML's samples were all mechanically conditioned and appeared very repeatable. While KUL did not mechanically condition their samples, they conducted the shear test three times on each fabric blank and noted a large difference between the 1st run and the 2nd and 3rd runs. However, there was not a large difference in the results when only comparing the 2nd and 3rd runs. Based on the results from numerical studies manufacturers may want to consider the incorporation of a step into the manufacturing process to mechanically condition the fabric blank.

Test results provided by different groups show consistency but still have some deviations. Further studies are underway to help develop a standard test setup and procedure for obtaining accurate and appropriate material properties. Material responses under different speeds and temperatures will be further investigated. Calibration, sample preparation, and other important techniques to increase the accuracy of the tests will be collected and shared among the community. High temperature tests present challenges to researchers as they limit the use of optical devices and require higher sensitivity of the testing equipment. However, these optical methods showed that determining the shear angle mathematically from the crosshead displacement was a reasonable method as the shear angles obtained optically using Aramis and AutoCad did not vary significantly from the method used to calculate the shear angle from the crosshead displacement.

It was noted that a direct comparison of the region immediately preceeding the locking angle and the region following the locking angle could not be made because all groups did not take the same amount of data. However, the fact that a complete comparison cannot be made at this time, does not diminish the

importance of this data. Researchers have learned that picture-frame test results obtained from different research groups using different sample and frame sizes are comparable and that the energy method for normalization appears to be the best method in the literature to date for normalizing picture-frame shear data. With the available data, the benchmarking research group can begin to use numerical methods, such as finite element analyses, to analyze the effects of fabric alignment, fabric conditioning and material type on the forming process. From the results of the numerical investigations, forming experiments can be judiciously chosen and performed to validate the numerical results.

13.6 Acknowledgements

The authors would like to thank NSF, Saint-Gobain, Inc., Hong Kong RGC (under grant HKUST6012/02E), the Netherlands Agency for Aerospace Programmes and a Marie Curie Fellowship of the EC (HPMT-CT-2000-00030).

The contributions of the following researchers are also acknowledged and sincerely appreciated: H.S. Cheng,[1] T.X. Yu,[2] B. Zhu,[2] X.M. Tao,[2a] S.V. Lomov,[3] Tz. Stoilova,[3] I.Verpoest,[3] P. Boisse,[4] J. Launay,[4] G. Hivet,[4] L. Liu,[5] E.F. de Graaf,[6] R. Akkerman[6]

1. Northwestern University – Dept. of Mech. Engng., Evanston, IL, 60208, USA.
URL:http://www.mech.northwestern.edu/ampl/home.html
e-mail: jcao@northwestern.edu
2. Hong Kong University of Science and Technology, Clear Water Bay, Kowloon, Hong Kong
URL:http://www.me.ust.hk.html
e-mail: metxyu@ust.hk
2a. Hong Kong Polytechnic University, Hung Hom, Kowloon, Hong Kong.
e-mail: tctaoxm@polyu.edu.hk
3. Katholieke Universiteit Leuven, Belgium
URL: http://www.mtm.kuleuven.ac.be/Research/C2/poly/index.htm
e-mail: Stepan.Lomov@mtm.kuleuven.ac.be
4. Laboratoire de Mécanique des Systèmes et des Procédés, France
e-mail: Philippe.Boisse@univ-orleans.fr
5. University of Massachusetts at Lowell, Dept of Mechanical Eng, Lowell, MA 01854 USA
URL: http://m-5.eng.uml.edu/acmtrl/
e-mail: Julie_Chen@uml.edu
6. University of Twente, Netherlands
URL: http://www.opm.ctw.utwente.nl/en/pt/
e-mail: R.Akkerman@ctw.utwente.nl

13.7 References and further reading

Cao, J., H.S. Cheng, T.X. Yu, B. Zhu, X.M. Tao, S.V. Lomov, Tz. Stoilova, I.Verpoest, P. Boisse, J. Launay, G. Hivet, L. Liu, J. Chen, E.F. de Graaf, R. Akkerman (2004). 'A Cooperative Benchmark Effort on Testing of Woven Composites', *ESAFORM 2004,* pp. 305–308.

Harrison, P., M.J. Clifford, A.C. Long (2004). 'Shear characterization of viscous woven textile composites: a comparison between picture frame and bias extension experiments', *Composites Science and Technology*, Vol. 64, pp. 1453–1465.

Lebrun, G., M.N. Bureau, J. Denault (2003). 'Evaluation of bias-extension and picture-frame test methods for the measurement of intraply shear properties of PP/glass commingled fabrics', *Composite Structures*, Vol. 61, pp. 341–352.

Lomov, S.V., Tz. Stoilova, I. Verpoest (2004). 'Shear of woven fabrics: Theoretical model, numerical experiments and full field strain measurements', *ESAFORM Conference 2004.*

Long, A.C., F. Robitaille, B.J. Souter (2001). 'Mechanical modeling of in-plane shear and draping for woven and non-crimp reinforcements', *Journal of Thermoplastic Composite Materials*, 14, pp. 316–326.

Lussier, D. (2000). 'Shear Characterization of Textile Composite Formability', Masters Thesis, Department of Mechanical Engineering at the University of Massachusetts Lowell.

Peng, X.Q., J. Cao, J. Chen, P. Xue, D.S. Lussier, L. Liu (2004). 'Experimental and numerical analysis on normalization of picture frame tests for composite materials', *Composites Science and Technology*, Vol. 64, pp. 11–21.